Supporting information

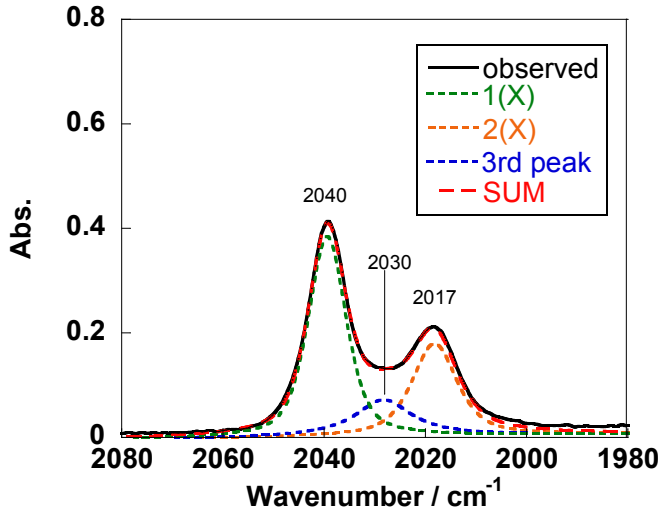

Figure S1. IR spectrum of *fac*-[Mn^{I}(bpy)$(CO)_3$(MeCN)]$^+$ measured in a DMF solution containing 3.9 M TEOA (black line) and each peaks of 1(H) (green broken line) and 2(H) (orange broken line) and 3rd component (blue broken line) obtained by curve fitting for observed spectra. Summation of these peak is shown as a red broken line.

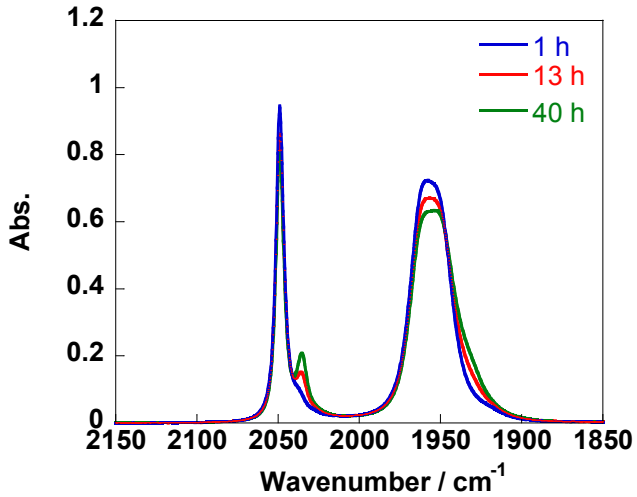

Figure S2. IR spectrum of *fac*-[Mn^{I}(bpy)$(CO)_3$(MeCN)]$^+$ measured in a MeCN-TEOA mixed solution after several hours from solving (a) or a DMF-MeCN-TEOA mixed solution after 2h from solving (b).

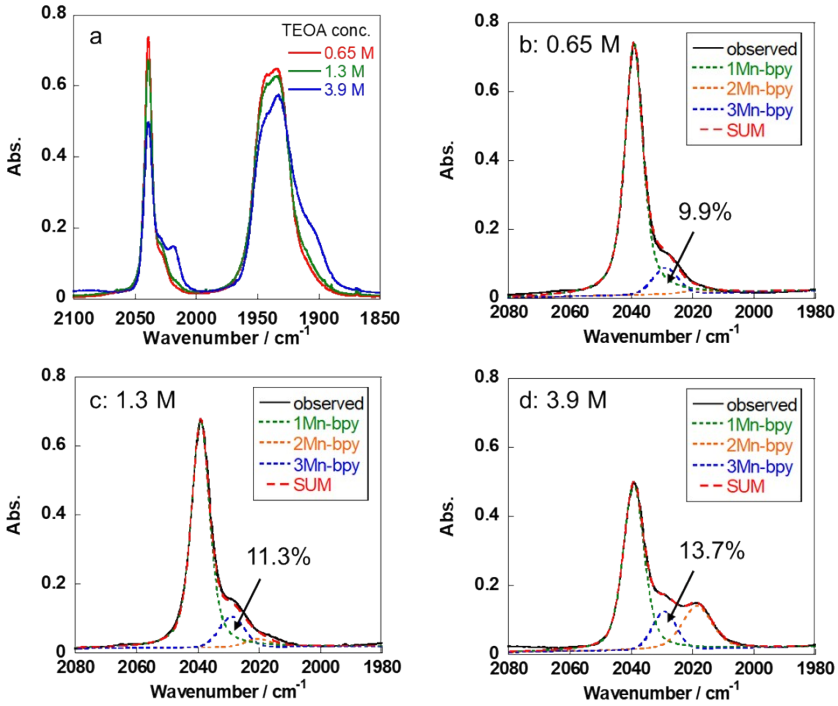

Figure S3. IR spectrum of *fac*-[Mn^{I}(bpy)(CO)$_3$(MeCN)]$^+$ measured in a DMF containing several concentrations of TEOA. *fac*-[Mn^{I}(bpy)(CO)$_3$(MeCN)]$^+$ was dissolved into a DMF solution containing 1.3 M of TEOA. After the solution was kept for 60 min, additional TEOA or DMF was added into the solution, i.e., the concentration of TEOA in the solution changed from 1.3 M to 3.9 M or 0.65 M, respectively.

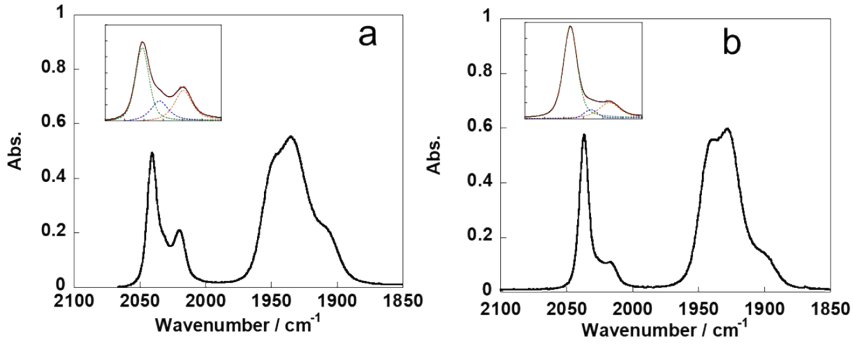

Figure S4. IR spectra of *fac*-[Mn^{I}(X$_2$bpy)(CO)$_3$(MeCN)]$^+$ (X = Br (a) or OMe (b)) in a DMF solution containing 3.8 M under Ar and curve fitting results (inset).

Table S1. K_1' of the Mn(I) and Re(I) complexes.

Metal	Mn(I)			Re(I)		
X	H	Br	OMe	H	Br	OMe
K_1'	0.66 (±0.06)	1.3 (±0.02)	0.46 (±0.01)	19	117 (±11)	27.3 (±2.2)

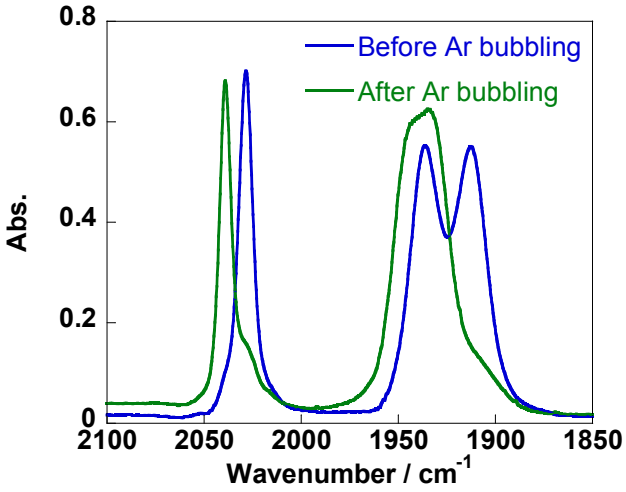

Figure S5. IR spectra of *fac*-[Mn^{I}(bpy)(CO)$_3$(MeCN)]$^+$ in a CO_2 saturated DMF-TEOA measured before (blue line) and after Ar bubbling (green line).

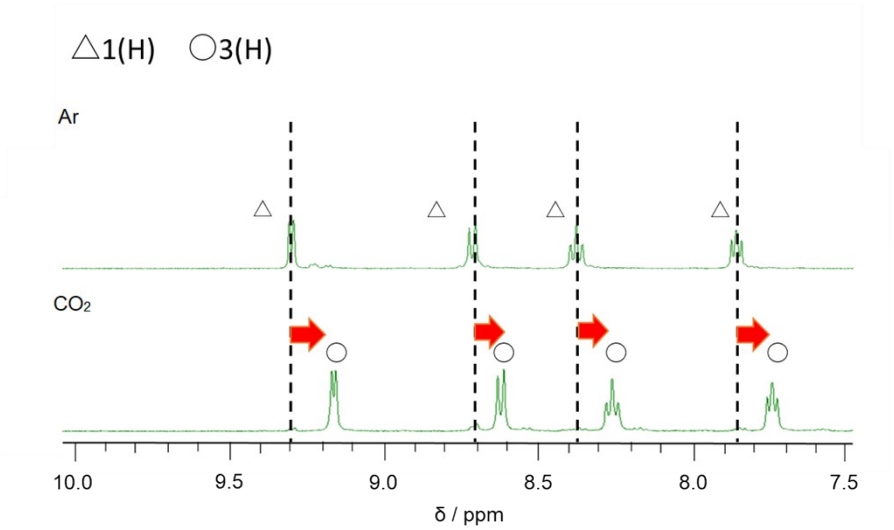

Figure S6. ^{1}H NMR spectra of *fac*-[Mn^{I}(bpy)(CO)$_3$(MeCN)]$^+$ in DMSO-d_6 containing 1.3 M TEOA under Ar (a) and CO_2 (b). **△1Mn-bpy**, **○4Mn-bpy**.

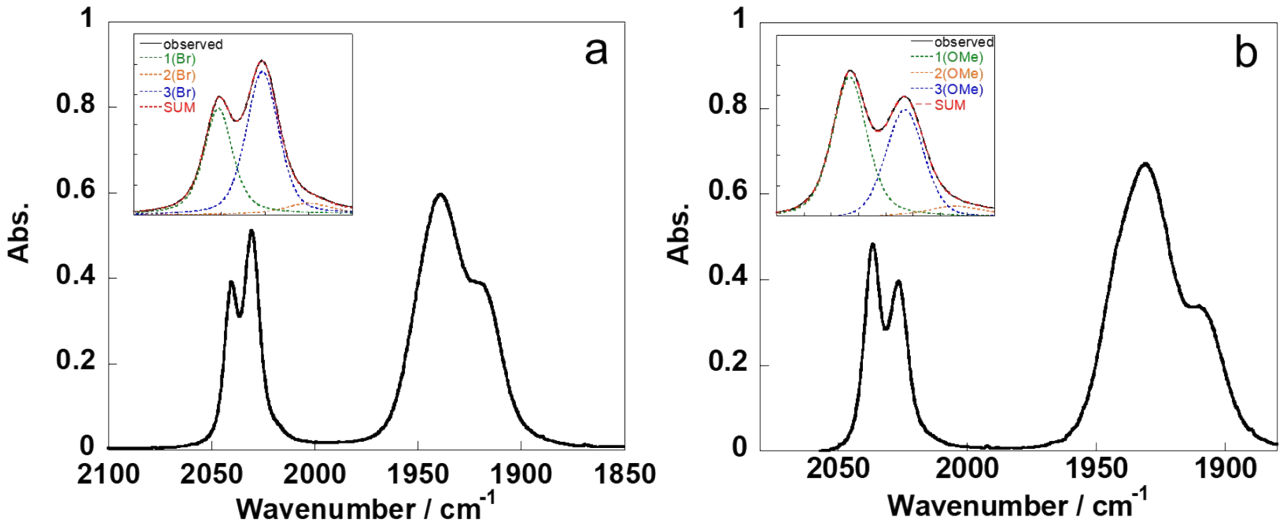

Figure S7. IR spectra of *fac*-[$Mn^{I}(X_2bpy)(CO)_3(MeCN)]^+$ (X = Br (a) or OMe (b)) in a DMF-TEOA mixed solution containing 3.17 mM CO_2.

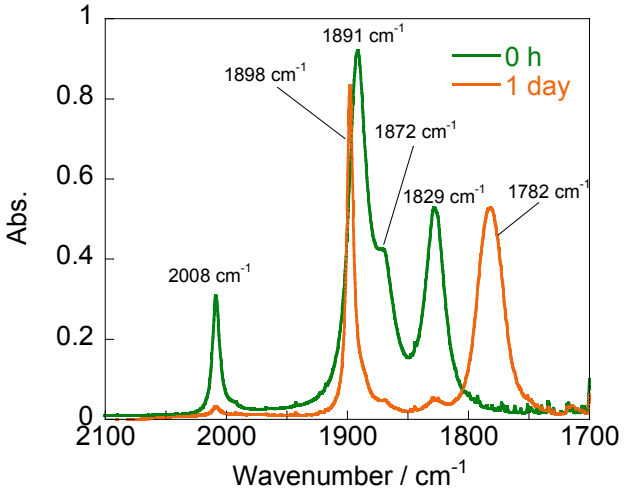

Figure S8. IR spectra of 4.9 mM [W(bpy)$(CO)_4$] in an acetonitrile solution before and after reflux for one day. ν_{co} at 2008, 1891, 1872 and 1829 cm^{-1} were of original species. After reflux, these peaks were almost completely disappeared and new bands at 1898 and 1782 cm^{-1} attributed to [W(bpy)$(CO)_3$(MeCN)] were observed.

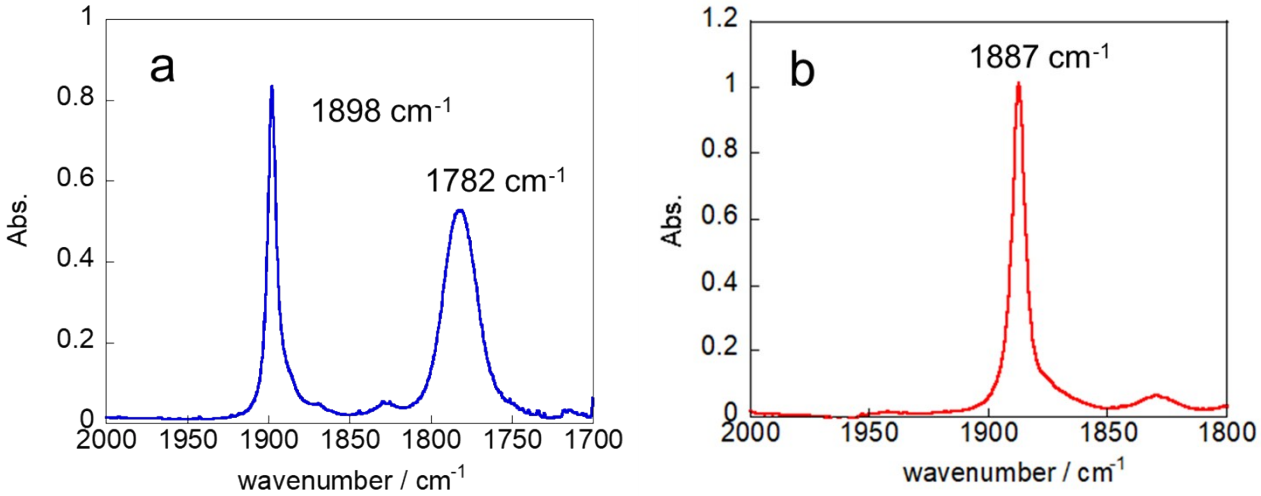

Figure S9. IR spectra of [W(bpy)$(CO)_3$(MeCN)] in an acetonitrile solution (a) or a DMF solution (b) In DMF, peak shift occurred to lower wavenumber than in MeCN most likely because MeCN on W(0) complex substituted to DMF.

Table S2. Selected bond lengths in the geometrically optimized structures for *fac*-Mn(I)(bpy)$(CO)_3$R and *fac*-Re(I)(bpy)$(CO)_3$R calculated at the def2-SVP/PBE1PBE level with PCM solvent model for DMF.

Mn(bpy) $(CO)_3$R				
	R			
	dmf	$OC_2H_4O(C_2H_5OH)_2$	$OCOOC_2H_4O(C_2H_5OH)_2$	I (exp) [a]
Mn-N1	2.056	2.055	2.058	2.03
Mn-N2	2.056	2.059	2.056	2.05
Mn-Oa	1.803	1.791	1.787	1.80

Mn-Oe	1.804	1.791	1.798	1.77
Mn-Oe	1.807	1.795	1.806	1.80
COa	1.142	1.151	1.149	1.15
COe1	1.145	1.150	1.148	1.19
COe	1.144	1.148	1.147	1.14
M-O(R)	2.075	2.020	2.045	2.724

Re(bpy) $(CO)_3R$				
	R			
	dmf	$OC_2H_4O(C_2H_5OH)_2$	$OCOOC_2H_4O(C_2H_5OH)_2$	$OCOOC_5H_{11}$ (exp) [b]
Re-N1	2.167	2.155	2.201	2.178
Re-N2	2.169	2.170	2.201	2.164
Re-Oa	1.903	1.904	1.911	1.898
Re-Oe	1.903	1.918	1.922	1.924
Re-Oe	1.925	1.928	1.926	1.921
COa	1.154	1.167	1.157	1.155
COe1	1.155	1.169	1.156	1.149
COe	1.159	1.168	1.154	1.146
M-O(R)	2.247	2.175	2.165	2.142

[a.] G. J. Stor, D. J. Stufkens, P . Vernooijs, E. J. Baerends, J. Fraanje, and K. Goubitzs, *Inorg. Chem.,* 34 (1995) 1588-1594

[b] M. K. Mbagu, D. N. Kebulu, A. Winstead, S. K. Pramanik, H. N. Banerjee, M. O. Iwunze, J. M. Wachira, G. E. Greco, G. K. Haynes, A. Sehmer, F. H. Sarkar, D. M. Ho, R. D. Pike, S. K. Mandal, *Inorg. Chem. Commun*., 21 (2012) 35–38.

Table S3. Calculated and observed ν(CO) vibrational wavenumbers of *fac*-Mn(bpy)$(CO)_3$R

R=$NCCH_3$		**R=dmf**		**R=TEOA**		**R=CO_2-TEOA**	
calcd	**obsd**	**calcd**	**obsd**	**calcd**	**obsd**	**calcd**	**obsd**
1989 (+44)	1945	1976 (+40)	1936	1950 (+48)	1902	1963 (+50)	1913
1998		1985 (+42)	1943	1960 (+42)	1918	1972 (+36)	1936
2077 (+31)	2046	2071 (+32)	2039	2050 (+33)	2017	2061 (+33)	2028

Values in parentheses denote the difference in frequency between the calculated and experimental.

Table S4. Calculated ν(CO) vibrational wavenumbers of *fac*-Mn(bpy)$(CO)_3$ TEOA(NH+)

R=TEOA(NH+)
calcd
1961
(+59)
1966
(+48)
2057
(+40)

Values in parentheses denote the difference in frequency between the calculated and the observed species (1902, 1918, and 2017 cm^{-1}).

Table S5. Calculated and observed ν(CO) vibrational wavenumbers of *fac*-Re(bpy)$(CO)_3$R

R=$NCCH_3$		**R=dmf**		**R=TEOA**		**R=CO_2-TEOA**	
calcd	**obsd**	**calcd**	**obsd**	**calcd**	**obsd**	**calcd**	**obsd**
1948		1934 (+21)	1913	1902 (+21)	1881	1915 (+23)	1892
1956 (+21)	1935	1938 (+16)	1922	1913 (+16)	1897	1928 (+13)	1915
2053 (+16)	2037	2047 (+18)	2029	2025 (+19)	2006	2038 (+18)	2020

Values in parentheses denote the difference in frequency between the calculated and experimental.

Figure S10. Molecular structures of *fac*-Mn(bpy)$(CO)_3$-TEOA(left) and *fac*-Mn(bpy)$(CO)_3$-CO_2-TEOA(right). The values in figures denote the length of hydrogen bonding.